EAI Endorsed Transactions
on Energy Web
Research Article EAI.EU

Unified Systems for Traction and Battery Charging of Electric Vehicles: A Sustainability Perspective

Tiago J. C. Sousa[1,*], Vítor Monteiro[1], Delfim Pedrosa[1], Luís Machado[1], João L. Afonso[1]

[1]ALGORITMI Research Centre, University of Minho, Guimaraes, Portugal

Abstract

This paper presents an analysis of unified systems for traction and battery charging of electric vehicles (EVs), regarding operation modes and implementation cost, when compared to dedicated systems that perform the same functionalities. Concerning the interface of the EV battery charging system with the power grid, four operation modes are analyzed: (1) grid-to-vehicle (G2V); (2) vehicle-to-grid (V2G); (3) vehicle-to-home (V2H); and (4) vehicle-for-grid (V4G), which, by using a unified system for traction and battery charging, can be linked both to single-phase and three-phase power grids. Moreover, a cost estimation is performed for EV unified systems and for dedicated systems that can perform the same functionalities when connected to the power grid, in order to prove the advantages of the system unification. The cost estimation is based on two power levels, namely 6 kW (single-phase), related to domestic installations and slow battery charging, and 50 kW (three-phase), related to industrial installations and fast battery charging. The relevance of unified systems for traction and battery charging of EVs is proven for single-phase and three-phase power grids both in terms of operationality and implementation cost.

Keywords: Electric Vehicle, Unified System, Smart Grids, Cost Estimation.

Received on 17 September 2020, accepted on 14 July 2021, published on 23 July 2021

doi: 10.4108/eai.23-7-2021.170557

1. Introduction

Electric vehicles (EVs) represent a growing alternative to the conventional fossil fuel powered vehicles towards the reduction of greenhouse emissions at the utilization level, as well as the refraining of fossil resources exploitation [1][2]. The conjugation of EVs and renewable energy sources represents one major role towards smart grids, with the bidirectional operation for EVs offering new operation modes and grid supporting functionalities [3]-[5] In this sense, the integration of EVs in the power grid has been a major research topic, since the EV can be seen as a mobile energy storage system for the smart grid. Hence, the typical EV battery charging operation (grid-to-vehicle – G2V) can be extended to the vehicle-to-grid (V2G) operation mode, initially proposed in [6]. In this operation mode, the EV is connected to the power grid and acts as a grid-tied inverter, i.e., injecting energy into the power grid by synthesizing a sinusoidal current in phase opposition with the power grid voltage. Furthermore, other operation modes for the EV have been proposed in the literature, such as vehicle-to-home (V2H), where the EV acts as a voltage source for an electrical installation, and vehicle-for-grid (V4G), where the EV acts as an active power conditioner, i.e., a shunt active power filter (SAPF) [7]-[11].

The referred functionalities are accomplished with an on-board EV battery charger, which is limited to power levels below 19.2 kW in the best-case scenario [12]. However, with integrated EV battery chargers, i.e., a unified system for traction and battery charging of an EV, higher power levels are achievable. This happens because the maximum power is dictated by the traction system nominal power, which is typically several dozens or few hundreds of kW for automobiles. Therefore, unified systems for traction and battery charging of EVs allow the battery charging operation with higher power levels, as well as the other referred operation modes. In this way, it

*Corresponding author. Email: tsousa@dei.uminho.pt

is possible to operate in industrial installations, for instance. Moreover, since all the referred operation modes are accomplished with a single system, the use of dedicated equipment for each operation can be discarded, e.g., load shift system (LSS) or SAPF. The first publication regarding unified systems for traction and battery charging of EVs dates back to 1983 in a joint work between the US Department of Energy and NASA [13][14]. However, in this work the traction system was sized to a peak power of 34 kW, while the battery charging operation was limited to a continuous power of 3.6 kW (single-phase). In the beginning of the 1990s, three unified systems were patented by Rippel and Cocconi [15]-[17]. The first two of these systems were able to interface only single-phase power grids, while the third one was capable of interfacing both single-phase and three-phase power grids. Besides the type of power grid to which the system can be connected, in the literature can also be found unified systems comprising galvanic isolation [18] and based on the machine winding reconfiguration [19]-[21], unified systems based on two [22] and four [23] electrical machines, unified systems for switched reluctance machines [24]-[29], unified systems for multiphase machines [30]-[33] and unified systems using the machine windings as coupling inductors to interface with the power grid [34][35]. This approach represents a major challenge, since electrical machines with nominal power levels for EV applications present low values of leakage inductance. This fact leads to the use of additional filters or the operation with higher switching frequencies. Besides, in order to use the machine windings as grid coupling inductors, it is mandatory to have access to all the machine winding terminals. Another issue regarding this approach is the fact that the machine is prone to rotate when the system operates in the battery charging mode. This happens if an asynchronous machine is used, since it is self-started, contrarily to synchronous machines that must be synchronized with the power supply in order to produce torque and, consequently, rotation. Therefore, a mechanical clutch should be used in order to disconnect the machine from the downstream traction system. On the other hand, the use of additional inductors increases the cost, volume and weight of the system. Besides, low value inductors should be used, since the combination of high inductance and high current characteristics gives rise to heavy and bulky inductors, which are not adequate for an EV. Therefore, the use of additional filters or the operation with higher switching frequencies is also a necessity.

In this context, this paper presents the advantages of unified traction and battery charging systems for EVs, both in terms of operation modes and in terms of implementation cost, when compared to dedicated solutions that perform the same operation modes. Hence, four operation modes are analyzed: (1) grid-to-vehicle (G2V); (2) vehicle-to-grid (V2G); (3) vehicle-to-home (V2H); and (4) vehicle-for-grid (V4G). With a unified system, each of these operation modes can be used in single-phase and three-phase power grids. Furthermore, a cost estimation is performed for a unified system and for dedicated systems that can perform the same functionalities, namely an LSS and a SAPF, in order to prove the benefits of the EV unified approach. The main goal of this paper is to evaluate the practical benefits of unified systems for traction and battery charging of EVs, since their feasibility in terms of implementation cost is not usually addressed in research studies.

This paper is an extended version of [36] and is structured as follows: Section 2 presents the operation modes under analysis, as well as simulation results of each one; Section 3 presents a cost estimation and comparison with conventional dedicated solutions; finally, Section 4 draws the conclusions of this paper.

2. Operation Modes

This section shows the operation modes considered for the EV in the scope of this paper, which are the following: (1) grid-to-vehicle (G2V); (2) vehicle-to-grid (V2G); (3) vehicle-to-home (V2H); and (4) vehicle-for-grid (V4G). All the referred operation modes encompass the connection of the EV to an electrical installation, which can be either single-phase or three-phase. Figure 1 shows a block diagram of the general connection of the EV to an electrical installation with the referred operation modes. It should be noted that all the operation modes take in consideration high levels of power quality, which is a relevant feature for smart grids. In the scope of this paper, only the front-end ac-dc converter operation is analyzed. It should be noted that the waveforms presented in this section correspond to simulation results obtained with the software PSIM v9.1, but have only illustrative purposes for helping to describe the different operation modes.

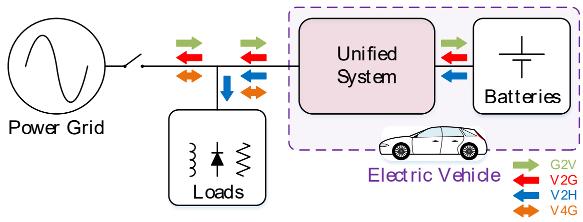

Figure 1. Block diagram of the EV connection to an ac electrical installation.

2.1. Grid-to-Vehicle (G2V)

The traditional operation of an on-board EV battery charger, i.e., charging the batteries with power provided by the power grid, is commonly referred as G2V. Figure 2 shows a block diagram of this operation mode. The battery charging performed by on-board EV battery chargers is typically classified as slow, since the power level of these systems is limited to 19.2 kW, as previously referred. On the other hand, by using a unified system for traction and battery charging, higher power levels can be used in the battery charging operation, hence equipping the EV with an on-board fast battery charger. With this system, both slow and fast battery charging are possible, which are accomplished by connecting the EV to single-phase and three-phase power grids, respectively.

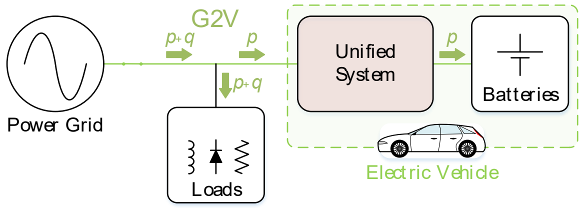

Figure 2. Block diagram of the Grid-to-Vehicle (G2V) operation mode.

In this operation mode, the amplitude of the power grid current is controlled in order to provide the necessary power to perform the battery charging, while also maintaining the dc-link voltage regulated accordingly to the established reference value. Moreover, the power grid current is controlled in order to be in phase with the power grid voltage and to present a sinusoidal waveform, even if the power grid voltage contains harmonic distortion. This is possible by using a phase-locked loop (PLL) algorithm, this way guaranteeing high levels of power quality from the power grid point of view, independently of the power level used for the battery charging.

When connected to a single-phase power grid, the reference current for the EV in the G2V operation mode (i_g^*) is given by:

$$i_g{}^* = \frac{P_{dc} + P_{bat}}{V_g^2} v_{g\_pll} \,, \qquad (1)$$

where P_{dc} is the average value of the power necessary to control the dc-link voltage to the established reference value, P_{bat} is the average value of the power necessary to perform the battery charging, V_g is the rms value of the power grid voltage and v_{g_pll} is the instantaneous value of the fundamental component of the power grid voltage, which is obtained through the PLL algorithm. The value of P_{dc} can be obtained from a proportional-integral (PI) controller, while P_{bat} can simply be obtained from the multiplication of the battery voltage and current. It is convenient that both power values are passed through a low-pass filter in order to mitigate oscillation which, in turn, would cause harmonic distortion in the reference current i_g^*.

When connected to a three-phase power grid, the reference current for phase x of the EV in the G2V operation mode (i_{gx}^*) is given by:

$$i_{g_x}{}^* = \frac{P_{dc} + P_{bat}}{v_{g_{a\_pll}}{}^2 + v_{g_{b\_pll}}{}^2 + v_{g_{c\_pll}}{}^2} v_{g_{x\_pll}} \,, \qquad (2)$$

where P_{dc} is the average value of the power necessary to control the dc-link voltage to the established reference value, P_{bat} is the average value of the power necessary to perform the battery charging, v_{gx_pll} is the instantaneous value of the fundamental component of the power grid voltage in phase x, with $x = \{a, b, c\}$, which is obtained through the PLL algorithm, and v_{ga_pll}, v_{gb_pll} and v_{gc_pll} are the same as v_{gx_pll} for phases a, b and c, respectively. The values of P_{dc} and P_{bat} can be obtained by the same way as in the single-phase case and, once again, it is convenient that both pass through a low-pass filter in order to mitigate oscillation which, in turn, would cause harmonic distortion in the reference currents i_{gx}^*.

Figure 3 shows a simulation result of this operation mode for an operating power of 3.2 kW (slow battery charging, single-phase), where it can be seen the power grid voltage (v_g) and current (i_g) and the dc-link voltage (v_{dc}). It can be seen that v_g is not sinusoidal, but the system is capable of absorbing a sinusoidal current i_g in phase with v_g, aiming for a practically unitary power factor. Besides, v_{dc} is controlled to the established reference average value of 400 V.

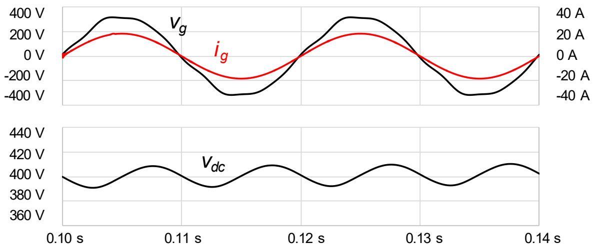

Figure 3. Simulation results of the G2V operation mode for a power of 3.2 kW (single-phase): Power grid voltage (v_g), power grid current (i_g) and dc-link voltage (v_{dc}).

In order to verify the fast battery charging capability of a unified system, Figure 4 shows a result of the G2V operation mode for an operating power of 50 kW (fast battery charging, three-phase), where the phase-neutral voltages (v_{ga}, v_{gb}, v_{gc}), the phase currents (i_{ga}, i_{gb}, i_{gc}) and the dc-link voltage (v_{dc}) can be seen. Also, in this case, each phase current is sinusoidal and in phase with the respective phase-neutral voltage, even if the voltage is not sinusoidal. In this case, v_{dc} is controlled to the established reference average value of 800 V.

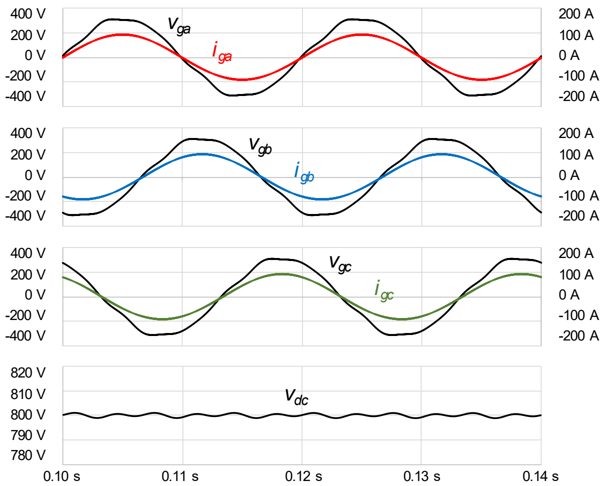

Figure 4. Simulation results of the G2V operation mode for a power of 50 kW (three-phase): Power grid voltages (v_{gx}), power grid currents (i_{gx}) and dc-link voltage (v_{dc}).

2.2. Vehicle-to-Grid (V2G)

The V2G operation mode consists in delivering energy, previously stored in the EV batteries, back to the power grid. This operation mode, whose block diagram can be seen in Figure 5, represents a promising benefit for smart grids in the sense that it endows the EV with auxiliary functions to the power grid. Moreover, the combination of G2V and V2G operation modes allows the EV to operate as an LSS. These functions can be accomplished with a conventional bidirectional on-board EV battery charger, with the main difference relatively to a unified system being the admissible power levels for operation. Therefore, the unified system considered in this paper encompasses the V2G operation mode both in single-phase and three-phase power grids, allowing grid support functionalities, for instance, in domestic and industrial electrical installations.

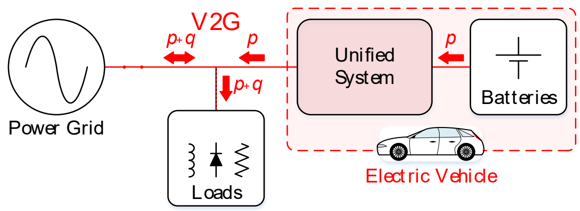

Figure 5. Block diagram of the Vehicle-to-Grid (V2G) operation mode.

In this operation mode, similarly to G2V, the amplitude of the power grid current is controlled in order to provide the necessary power to perform the energy injection into the power grid while also maintaining the dc-link voltage regulated accordingly to the established reference value. Moreover, the power grid current is controlled in order to be in phase opposition with the power grid voltage and to present a sinusoidal waveform, even if the power grid voltage contains harmonic distortion. Once again, this is possible by using a PLL algorithm, guaranteeing high levels of power quality from the power grid point of view, independently of the power level used for the energy injection. The equations used in the G2V operation mode (equations (1) and (2)) are valid for the V2G operation mode, with the difference being that the value of P_{bat} is negative, meaning that the batteries are acting as a power source instead of a load.

Figure 6 shows a simulation result of the V2G operation mode for an operating power of 3.2 kW (single-phase), which can be accomplished with almost any bidirectional battery charger. In this case, the power grid current (i_g) is also sinusoidal, but in phase opposition with the power grid voltage (v_g), meaning that the EV battery charger is operating as a power source. Besides, the phase shift between these two quantities is practically 180º, meaning a practically unitary power factor.

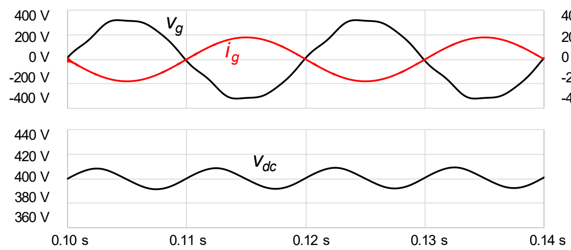

Figure 6. Simulation results of the V2G operation mode for a power of 3.2 kW (single-phase): Power grid voltage (v_g), power grid current (i_g) and dc-link voltage (v_{dc}).

Similarly to the previous case, the V2G operation mode can be performed in three-phase power grids, for higher power levels. Figure 7 shows this operation with a power of 50 kW (three-phase), where it can be seen the phase-neutral voltages (v_{ga}, v_{gb}, v_{gc}), the phase currents (i_{ga}, i_{gb}, i_{gc}) and the dc-link voltage (v_{dc}). Once again, the injected currents are sinusoidal and in phase opposition with the respective voltages, aiming for a unitary power factor.

2.3. Vehicle-to-Home (V2H)

The V2H operation mode, whose block diagram can be seen in Figure 8, consists in the EV acting as a voltage source for the electrical installation, disconnecting the installation from the upstream grid and supplying the loads with energy stored in the EV batteries. This operation mode can be initiated either in a planned way, such as in LSSs, or triggered by disturbances in the power grid voltage, i.e., overvoltages or undervoltages, similarly to an off-line uninterruptible power supply (UPS). Therefore, by comprising unified systems for traction and battery charging, EVs can act as off-line UPSs in both domestic and industrial installations, which can avoid the use of dedicated UPSs when the EV is parked.

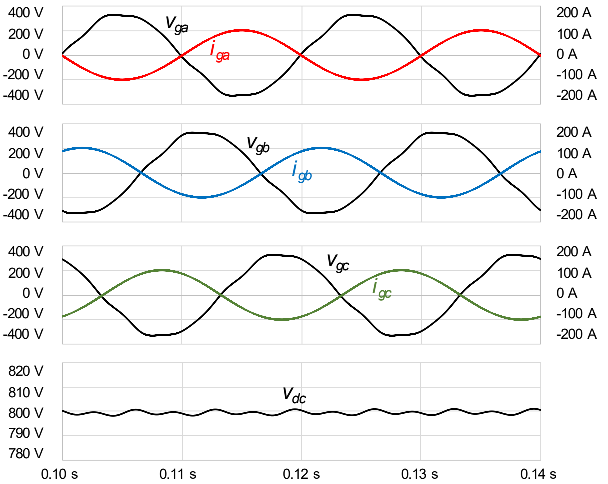

Figure 7. Simulation results of the V2G operation mode for a power of 50 kW (three-phase): Power grid voltages (v_{gx}), power grid currents (i_{gx}) and dc-link voltage (v_{dc}).

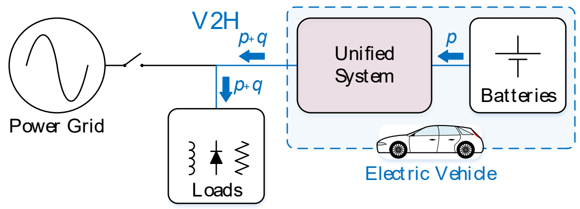

Figure 8. Block diagram of the Vehicle-to-Home (V2H) operation mode.

Contrarily to the operation modes previously presented in this paper, the V2H operation mode uses a reference voltage instead of a reference current. Independently of the trigger of this operation mode (planned or backup), the reference voltage uses predefined values of rms voltage and frequency, which in this case are 230 V and 50 Hz, respectively, in order to comply with the power grid in which the EV is connected. Nevertheless, these values could be adjusted in order to accommodate other types of ac power grids. Besides the rms value and frequency, care must be taken regarding the phase angle of the reference voltage, which is especially relevant regarding the backup (UPS) operation. For this purpose, the phase angle obtained from the PLL algorithm can be used for the reference voltage in the V2H operation mode, making the transition to this operation mode as seamless as possible when triggered by a disturbance, as an off-line UPS should guarantee. Regarding the V2H planned startup, i.e., as in an LSS, a seamless transition is not as relevant, as long as the supplied loads are not critical loads. Nonetheless, even if critical loads are used, a simple zero-crossing detection mechanism is sufficient to initiate the V2H operation mode smoothly.

Figure 9 shows the V2H operation mode initiated in a planned way, similarly to an LSS when used for self-consumption (single-phase). As it can be seen, the EV battery charger produces a 230 V, 50 Hz ac voltage (v_{ev}) that is practically sinusoidal even with a distorted current consumption (i_{ev}), which is drawn by a linear RL load and a nonlinear diode bridge rectifier with capacitive filter, absorbing a combined power of 5.3 kW. For this operation, due to the increased ripple in the dc-link voltage (v_{dc}) as a consequence of distorted current consumption (approximately 40 V peak-to-peak in this case), its reference value was slightly increased compared to the previous reference value of 400 V, hereby being established the value of 450 V.

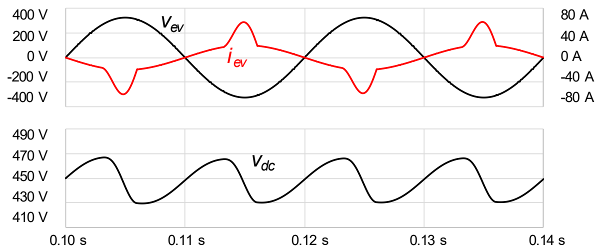

Figure 9. Simulation results of the V2H operation mode for a power of 5.3 kW (single-phase): Produced ac voltage (v_{ev}), absorbed current (i_{ev}) and dc-link voltage (v_{dc}).

Figure 10 shows the V2H operation mode for three-phase installations, with an operating power of 30 kW drawn by the same two types of load as the previous case. This figure shows the produced ac voltages (v_{eva}, v_{evb}, v_{evc}), the respective consumed currents (i_{eva}, i_{evb}, i_{evc}) and the dc-link voltage (v_{dc}). Similarly to the previous case, the produced voltages are sinusoidal with the desired amplitude even with distorted current consumption.

2.4. Vehicle-for-Grid (V4G)

The V4G operation mode consists in the compensation of power quality problems to the electrical installation where the vehicle is connected to. This operation mode can be performed simultaneously with either the operation modes G2V or V2G, as the bidirectional arrows of Figure 11 suggest. The main difference between the V4G and the regular G2V or V2G operation modes resides in the current, absorbed or injected from the power grid. The current is sinusoidal in G2V and V2G operation modes, while in V4G the purpose is to guarantee a sinusoidal grid current and in phase with the voltage, i.e., with the EV acting as a SAPF. Once again, with a unified system, this operation mode can be accomplished in single-phase and three-phase installations, allowing power conditioning functionalities in both domestic and industrial facilities.

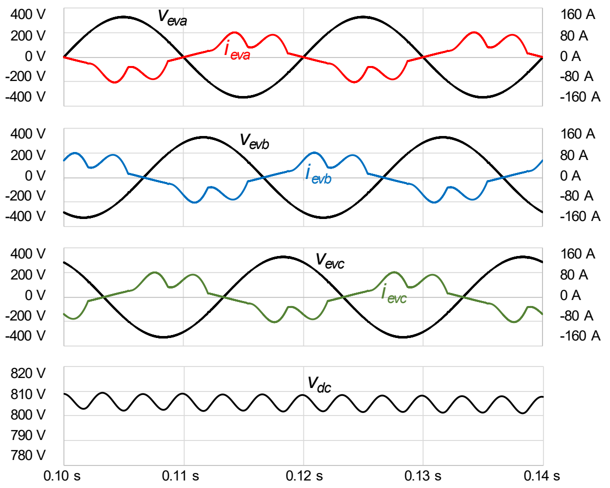

Figure 10. Simulation results of the V2H operation mode for a power of 30 kW (three-phase): Produced ac voltages (v_{evx}), absorbed currents (i_{evx}) and dc-link voltage (v_{dc}).

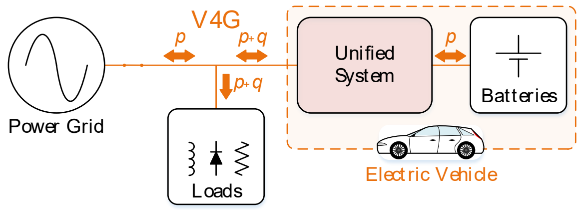

Figure 11. Block diagram of the Vehicle-for-Grid (V4G) operation mode.

Since the EV acts as a SAPF in the V4G operation mode, a power theory must be used in order to generate a reference current for the EV capable of compensating the power quality problems regarding the currents, i.e., harmonics and reactive power. It should be referred that, for three-phase operation, only three-wire systems were considered, so the compensation of current unbalances is not addressed in this paper. Both for single-phase and three-phase power grids it was considered the Fryze-Buchholz-Depenbrock (FBD) power theory, which consists of replacing the loads by their equivalent conductance connected in parallel with a current source. According to this power theory, the equivalent conductance represents the active power drawn by the loads, while the current source represents the harmonic currents and reactive power consumed by them [37]. Thus, the SAPF must generate the component of the loads current represented by the current source, while the power grid supplies the load solely with the equivalent conductance component, i.e., the loads are seen by the power grid as linear, consuming sinusoidal currents in phase with the respective power grid voltages. Therefore, the current that the EV must produce in order to guarantee the V4G and G2V/V2G operation modes combined in single-phase power grids ($i_{ev}{}^{*}$) is given by:

$$i_{ev}{}^{*} = \frac{P_{ld} + P_{dc} + P_{bat}}{V_g^2} v_{g\_pll} - i_{ld} \,, \tag{3}$$

where P_{ld} is the active power consumed by the loads, P_{dc} is the average value of the power necessary to control the dc-link voltage to the established reference value, P_{bat} is the average value of the power necessary to perform the battery charging (positive P_{bat}, for operation in G2V) or discharging (negative P_{bat}, for operation in V2G), V_g is the rms value of the power grid voltage, v_{g_pll} is the instantaneous value of the fundamental component of the power grid voltage, which is obtained through the PLL algorithm, and i_{ld} is the instantaneous value of the current consumed by the loads. As it can be seen, equation (3) is very similar to equation (1) regarding G2V/V2G operation modes, essentially containing an extra power component concerning the loads and the load current, whose subtraction with the sinusoidal component of the equation will result in the harmonic currents and reactive power consumed by the loads. As previously referred regarding P_{dc} and P_{bat}, the power component P_{ld} must be passed through a low-pass filter in order to allow the operation of the system with sinusoidal grid current.

When connected to a three-phase power grid, the current that the EV must produce in phase x in order to guarantee the V4G and G2V/V2G operation modes combined in three-phase power grids ($i_{evx}{}^{*}$) is given by:

$$i_{ev_x}{}^{*} = \frac{P_{ld_x} + P_{dc} + P_{bat}}{v_{g_{a\_pll}}{}^2 + v_{g_{b\_pll}}{}^2 + v_{g_{c\_pll}}{}^2} v_{g_{x\_pll}} - i_{ld_x} \,, \tag{4}$$

where P_{ldx} is the active power consumed by the loads in phase x, P_{dc} is the average value of the power necessary to control the dc-link voltage to the established reference value, P_{bat} is the average value of the power necessary to perform the battery charging (positive P_{bat}, for operation in G2V) or discharging (negative P_{bat}, for operation in V2G), v_{gx_pll} is the instantaneous value of the fundamental component of the power grid voltage in phase x, with $x = \{a, b, c\}$, which is obtained through the PLL algorithm, and v_{ga_pll}, v_{gb_pll} and v_{gc_pll} are the same as v_{gx_pll} for phases a, b and c, respectively. Once again, equation (4) is very similar to equation (2), i.e., regarding G2V/V2G operation modes, with the differences being the same as the ones previously pointed for single-phase power grids.

Figure 12 shows the V4G operation mode in single-phase installations for two different scenarios, with Figure 12 (a) showing the combination of V4G and G2V and Figure 12 (b) showing the combination of V4G and V2G. In both cases, the connected loads (a linear RL and a nonlinear diode bridge rectifier with capacitive filter) present a power consumption of 1.5 kW. Both figures show the power grid voltage (v_g), the load current (i_{ld}), the current produced by the EV battery charger (i_{ev}), the resulting grid current (i_g) and the dc-link voltage (v_{dc}).

In Figure 12 (a), the EV batteries are being charged with a power of 3 kW. In order to perform the V4G operation, the current absorbed by the EV battery charger is not sinusoidal, but contains the necessary harmonic distortion to obtain a sinusoidal current from the power grid point of view. As it can be seen, the current i_g is sinusoidal and in phase with the voltage v_g.

In Figure 12 (b), the EV batteries are being discharged with a power of 3 kW. Once again, the current injected by the EV battery charger is not sinusoidal in order to perform the V4G operation. As it can be seen, the current i_g is sinusoidal and in phase opposition with v_g, meaning that energy is being delivered into the power grid with unitary power factor. This happens because the power delivered by the EV battery charger is higher than the power consumed by the loads, otherwise the resulting current i_g would be in phase with v_g, i.e., the power grid would have to provide the power difference to supply the loads. Hence, the power grid is absorbing 1.5 kW.

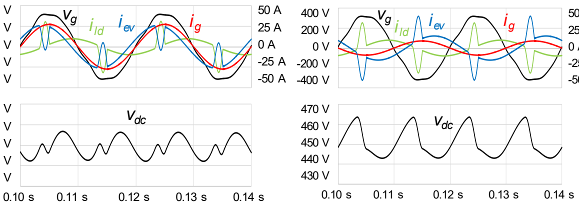

Figure 12. Simulation results of the V4G operation mode (single-phase), with 3 kW battery power and 1.5 kW load power, combined with: (a) G2V; (b) V2G.

Figure 13 shows the same operation mode in a three-phase power grid, where it can be seen the power grid voltages (v_{ga}, v_{gb}, v_{gc}), the load currents (i_{lda}, i_{ldb}, i_{ldc}), the currents produced by the EV battery charger (i_{eva}, i_{evb}, i_{evc}), the resulting grid currents (i_{ga}, i_{gb}, i_{gc}) and the dc-link voltage (v_{dc}). In both cases, the loads absorb a power of 10 kW.

Figure 13 (a) shows the combination of V4G and G2V operation modes, where the EV batteries are being charged with 30 kW. As it can be seen, the EV battery charger consumes distorted currents so that the power grid currents are sinusoidal and in phase with the respective voltages.

Figure 13 (b) shows the combination of V4G and V2G operation modes, where the EV batteries are being discharged with 30 kW. Once again, the currents produced by the EV battery charger are distorted, turning the power grid currents sinusoidal and in phase opposition with the respective voltages. Since the EV battery charger delivers 30 kW and the loads absorb 10 kW, the power grid is receiving 20 kW, therefore its currents are in phase opposition with the corresponding voltages.

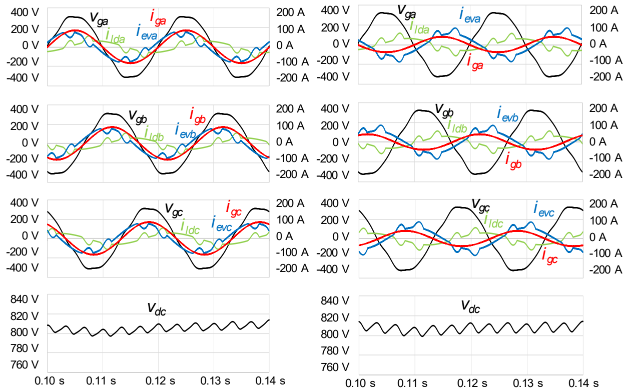

Figure 13. Simulation results of the V4G operation mode (three-phase), with 30 kW battery power and 10 kW load power, combined with: (a) G2V; (b) V2G.

3. Cost Comparison with Conventional Solutions

This section presents a comparison of an EV equipped with a unified system for traction and battery charging with the conventional dedicated systems for performing the abovementioned functionalities. Hence, an average cost estimation of a LSS and a SAPF is performed for two power ratings, namely 6 kW (single-phase) and 50 kW (three-phase), in order to compare with the slow and fast EV battery charging operation, respectively.

In terms of power electronics converters, a SAPF basically comprises an ac-dc converter. On the other hand, a LSS comprises the same structure, plus a dc-dc converter and the energy storage elements that are indispensable in a LSS, mostly based on lead acid or li-ion batteries [38]-[41]. However, the storage elements were discarded from the cost estimation, since that would require a more detailed and complex analysis regarding EVs.

Thereupon, Table 1 shows the cost estimation of the ac-dc and dc-dc power converters necessary to implement 6 kW single-phase LSS and SAPF systems, while Table 2 shows the analogous information regarding 50 kW three-phase systems. The information contained in these tables is depicted in Figure 14 for a SAPF (red) and an LSS (blue), for a 6 kW power rating in Figure 14 (a) and for a 50 kW power rating in Figure 14 (b). Besides, Table 3 shows the cost estimation of a 50 kW EV unified system, where it can be seen the minimum and maximum prices considered and the subsequent average value. It should be referred that the presented cost values are average values of a wide value range, since a power converter cost can depend on the topology of implementation, semiconductor approach, type of sensors, capacitor technology, among others. Besides, the prices vary with the retailer and with the quantity, with small quantities being considered in this case. As it can be seen, the LSS power stage has a slightly higher cost due to the additional dc-dc converter to interface the ac-dc converter dc-link with the energy storage system. The cost estimation of the power converters for a 50 kW LSS is also valid for an EV unified system, since the structure is the same.

Table 1. Cost estimation of the 6 kW single-phase power converters.

Component	Average price ac-dc converter	Average price dc-dc converter
Semiconductors	30 €	30 €
Drivers	50 €	50 €
Capacitors	400 €	50 €
Inductors	60 €	30 €
Sensors	50 €	30 €
Contactors	60 €	60 €
Total price	**650 €**	**250 €**

Table 2. Cost estimation of the 50 kW three-phase power converters.

Component	Average price ac-dc converter	Average price dc-dc converter
Semiconductors	200 €	100 €
Drivers	120 €	120 €
Capacitors	600 €	50 €
Inductors	500 €	500 €
Sensors	100 €	50 €
Contactors	350 €	350 €
Total price	**1870€**	**1170 €**

Table 3. Cost estimation of the 50 kW EV unified system.

Component	Minimum price	Maximum price	Average price
Semiconductors	200 €	400 €	300 €
Drivers	60 €	400 €	230 €
Capacitors	200 €	1 000 €	600 €
Inductors	800 €	1 200 €	1 000 €
Sensors	100 €	220 €	160 €
Contactors	300 €	1 200 €	750 €
Total price	**1660 €**	**4420 €**	**3040 €**

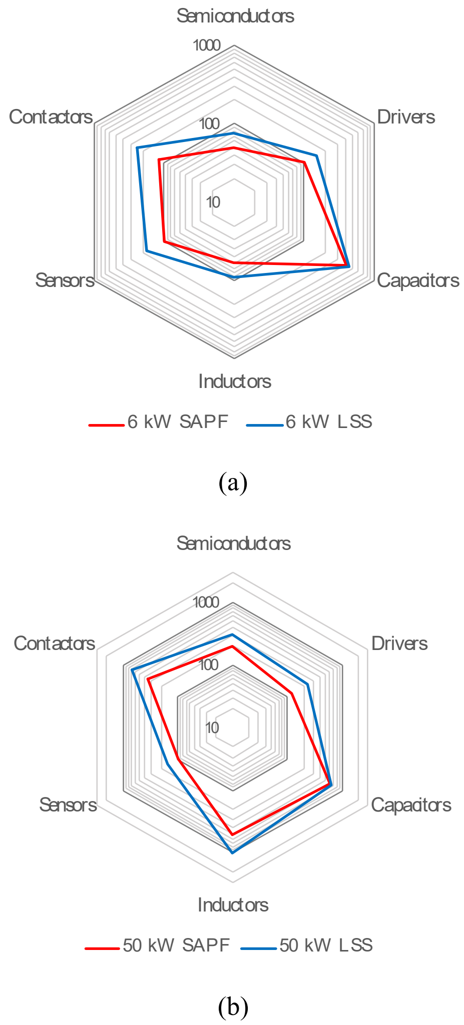

Figure 14. Cost estimation (in Euros) of the power electronics converters for a SAPF (red) and for an LSS (blue) considering a power rating of: (a) 6 kW (single-phase); (b) 50 kW (three-phase).

The total cost estimation of the power electronics converters for a SAPF, LSS and EV unified system can be seen in Table 4, both for 6 kW and 50 kW. As previously referred, the LSS and the EV unified system present the same average cost, which is the higher cost in the table (3 040 €). However, the EV can perform the same functionalities of the SAPF for the same power, without adding extra 1 870 €, besides being able to operate as a UPS. Moreover, the EV unified system can be seen as a mobile power electronics system, for instance, operating at home during the night and operating in a higher power installation during the day (i.e., at work), being able to perform the functionalities of two separate systems.

From this, it can be seen that the EV has an important role in power grids, being able to concentrate several operation modes in a single equipment, and it has even more relevance when a unified traction and battery charging system is used. It should be noted that this analysis only concerns the acquisition costs of the power electronics converters, not considering the battery costs. Besides, the analysis does not consider the investment payback that can be attained (e.g., with load shift operation), neither considers battery aging, which is a relevant issue in EVs. Nevertheless, the investment of an EV is already advantageous, both economically, environmentally and for the power grid, as long as its battery charger is capable of operating with good characteristics (i.e., sinusoidal current and bidirectional operation), and it can be even more advantageous when renewable energy sources are integrated. Accordingly, the advantages of the EV can be extended from households to industrial facilities if its EV battery charger is able to operate with higher power levels, i.e., by using a unified traction and battery charging system.

Table 4. Total cost estimation of the SAPF, LSS and EV unified system.

	Single-phase (6 kW)	Three-phase (50 kW)
SAPF	650 €	1 870 €
LSS	900 €	3 040 €
Unified System	-	3 040 €

4. Conclusions

This paper presented an analysis of unified systems for traction and battery charging of electric vehicles (EVs) in terms of operation modes and implementation cost when compared to dedicated systems that perform the same functionalities. Considering the connection of the system to the power grid, four operation modes were analyzed: (1) grid-to-vehicle (G2V); (2) vehicle-to-grid (V2G); (3) vehicle-to-home (V2H); and (4) vehicle-for-grid (V4G). By using a unified system for traction and battery charging, each of these operation modes can be performed both in single-phase and three-phase power grids, and in this paper, simulation results verified the correct operation of each mode. Furthermore, a cost estimation was performed, comparing the unified system with dedicated systems that perform the same functionalities, namely a load shift system (LSS) and a shunt active power filter (SAPF), for two power levels: 6 kW (single-phase), related to domestic installations and slow battery charging operation; and 50 kW (three-phase), related to industrial installations and fast battery charging operation. Both the cost estimation and the different possible operation modes prove that an EV with a unified system can play a relevant role in the power grid, both in single-phase and three-phase power grids, which is an attractive feature considering the paradigm of smart grids.

Acknowledgements.

This work has been supported by FCT – Fundação para a Ciência e Tecnologia within the Project Scope: UID/CEC/00319/2019. This work has been supported by the FCT Project DAIPESEV PTDC/EEI-EEE/30382/2017, and by FCT Project newERA4GRIDs PTDC/EEI EEE/30283/2017. Mr. Tiago J. C. Sousa is supported by the doctoral scholarship SFRH/BD/134353/2017 granted by the Portuguese FCT agency.

References

[1] C. C. Chan and Y. S. Wong, “Electric vehicles charge forward,” *IEEE Power and Energy Magazine*, vol. 2, no. 6, pp. 24–33, Nov. 2004.

[2] J. Milberg and A. Schlenker, “Plug into the Future,” *IEEE Power and Energy Magazine*, vol. 9, no. 1, pp. 56–65, Jan. 2011.

[3] J. Ansari, A. Gholami, A. Kazemi, and M. Jamei, “Environmental/economic dispatch incorporating renewable energy sources and plug-in vehicles,” *IET Generation, Transmission & Distribution*, vol. 8, no. 12, pp. 2183–2198, Dec. 2014.

[4] K. Knezovic, S. Martinenas, P. B. Andersen, A. Zecchino, and M. Marinelli, “Enhancing the Role of Electric Vehicles in the Power Grid: Field Validation of Multiple Ancillary Services,” *IEEE Transactions on Transportation Electrification*, vol. 3, no. 1, pp. 201–209, 2017.

[5] H. N. T. Nguyen, C. Zhang, and J. Zhang, “Dynamic Demand Control of Electric Vehicles to Support Power Grid With High Penetration Level of Renewable Energy,” *IEEE Transactions on Transportation Electrification*, vol. 2, no. 1, pp. 66–75, Mar. 2016.

[6] W. Kempton and J. Tomić, “Vehicle-to-grid power implementation: From stabilizing the grid to supporting large-scale renewable energy,” *Journal of Power Sources*, vol. 144, no. 1, pp. 280–294, 2005.

[7] V. Monteiro, J. G. Pinto, and J. L. Afonso, “Operation Modes for the Electric Vehicle in Smart Grids and Smart Homes: Present and Proposed Modes,” *IEEE Transactions on Vehicular Technology*, vol. 65, no. 3, pp. 1007–1020, Mar. 2016.

[8] V. Monteiro, B. Exposto, J. C. Ferreira, and J. L. Afonso, “Improved Vehicle-to-Home (iV2H) Operation Mode: Experimental Analysis of the Electric Vehicle as Off-Line UPS,” *IEEE Transactions on Smart Grid*, vol. 8, no. 6, pp. 2702–2711, 2017.

[9] S. Su *et al.*, “Reactive power compensation using electric vehicles considering drivers’ reasons,” *IET Generation, Transmission & Distribution*, vol. 12, no. 20, pp. 4407–4418, Nov. 2018.

[10] M. Kesler, M. C. Kisacikoglu, and L. M. Tolbert, “Vehicle-to-Grid Reactive Power Operation Using Plug-In Electric Vehicle Bidirectional Offboard Charger,” *IEEE Transactions on Industrial Electronics*, vol. 61, no. 12, pp. 6778–6784, Dec. 2014.

[11] R. Hou and A. Emadi, “Applied Integrated Active Filter Auxiliary Power Module for Electrified Vehicles With Single-Phase Onboard Chargers,” *IEEE Transactions on Power Electronics*, vol. 32, no. 3, pp. 1860–1871, Mar. 2017.

[12] M. Yilmaz and P. T. Krein, “Review of Battery Charger Topologies, Charging Power Levels, and Infrastructure for Plug-In Electric and Hybrid Vehicles,” *IEEE Transactions*

on Power Electronics, vol. 28, no. 5, pp. 2151–2169, May 2013.
[13] D. Thimmesch, "Integral Inverter/Battery Charger for Use in Electric Vehicles," USA Department of Energy/NASA, 1983.
[14] D. Thimmesch, "An SCR Inverter with an Integral Battery Charger for Electric Vehicles," *IEEE Transactions on Industry Applications*, vol. IA-21, no. 4, pp.1023–1029, Jul. 1985.
[15] W. Rippel, "Integrated traction inverter and battery charger apparatus," US4920475A, 1990.
[16] W. Rippel and A. Cocconi, "Integrated motor drive and recharge system," US5099186A, 1992.
[17] A. Cocconi, "Combined motor drive and battery charger system," US5341075A, 1994.
[18] F. Lacressonniere and B. Cassoret, "Converter used as a battery charger and a motor speed controller in an industrial truck," in *2005 European Conference on Power Electronics and Applications*, 2005, vol. 9, pp.P1–P7.
[19] S. Haghbin, S. Lundmark, M. Alakula, and O. Carlson, "An Isolated High-Power Integrated Charger in Electrified-Vehicle Applications," *IEEE Transactions on Vehicular Technology*, vol. 60, no. 9, pp.4115–4126, Nov. 2011.
[20] S. Haghbin, S. Lundmark, M. Alakula, and O. Carlson, "Grid-Connected Integrated Battery Chargers in Vehicle Applications: Review and New Solution," *IEEE Transactions on Industrial Electronics*, vol. 60, no. 2, pp.459–473, Feb. 2013.
[21] S. Haghbin, K. Khan, S. Zhao, M. Alakula, S. Lundmark, and O. Carlson, "An Integrated 20-kW Motor Drive and Isolated Battery Charger for Plug-In Vehicles," *IEEE Transactions on Power Electronics*, vol. 28, no. 8, pp.4013–4029, Aug. 2013.
[22] D.-G. Woo, D.-M. Joo, and B.-K. Lee, "On the Feasibility of Integrated Battery Charger Utilizing Traction Motor and Inverter in Plug-In Hybrid Electric Vehicles," *IEEE Transactions on Power Electronics*, vol. 30, no. 12, pp.7270–7281, Dec. 2015.
[23] Seung-Ki Sul and Sang-Joon Lee, "An integral battery charger for four-wheel drive electric vehicle," *IEEE Transactions on Industry Applications*, vol. 31, no. 5, pp.1096–1099, 1995.
[24] C. Pollock and Weng Kwai Thong, "Low-cost battery-powered switched reluctance drives with integral battery-charging capability," *IEEE Transactions on Industry Applications*, vol. 36, no. 6, pp.1676–1681, 2000.
[25] Development of a Compact Switched-Reluctance Motor Drive for EV Propulsion With Voltage-Boosting and PFC Charging Capabilities," *IEEE Transactions on Vehicular Technology*, vol. 58, no. 7, pp.3198–3215, Sep. 2009.
[26] An Integrated Driving/Charging Switched Reluctance Motor Drive Using Three-Phase Power Module," *IEEE Transactions on Industrial Electronics*, vol. 58, no. 5, pp.1763–1775, May 2011.
[27] Yihua Hu, Xueguan Song, Wenping Cao, and Bing Ji, "New SR Drive With Integrated Charging Capacity for Plug-In Hybrid Electric Vehicles (PHEVs)," *IEEE Transactions on Industrial Electronics*, vol. 61, no. 10, pp.5722–5731, Oct. 2014.
[28] Y. Hu, C. Gan, W. Cao, C. Li, and S. Finney, "Split Converter-Fed SRM Drive for Flexible Charging in EV/HEV Applications," *IEEE Transactions on Industrial Electronics*, vol. 62, no. 10, pp.6085–6095, Oct. 2015.
[29] K. W. Hu, P. H. Yi, and C. M. Liaw, "An EV SRM Drive Powered by Battery/Supercapacitor with G2V and V2H/V2G Capabilities," *IEEE Transactions on Industrial Electronics*, vol. 62, no. 8, pp.4714–4727, 2015.
[30] I. Subotic, N. Bodo, and E. Levi, "An EV Drive-Train with Integrated Fast Charging Capability," *IEEE Transactions on Power Electronics*, vol. 31, no. 2, pp.1461–1471, 2016.
[31] I. Subotic, N. Bodo, and E. Levi, "Single-phase on-board integrated battery chargers for EVs based on multiphase machines," *IEEE Transactions on Power Electronics*, vol. 31, no. 9, pp.6511–6523, 2016.
[32] V. Katic, I. Subotic, N. Bodo, E. Levi, B. Dumnic, and D. Milicevic, "Overview of fast on-board integrated battery chargers for electric vehicles based on multiphase machines and power electronics," *IET Electric Power Applications*, vol. 10, no. 3, pp.217–229, Mar. 2016.
[33] I. Subotic, N. Bodo, E. Levi, M. Jones, and V. Levi, "Isolated Chargers for EVs Incorporating Six-Phase Machines," *IEEE Transactions on Industrial Electronics*, vol. 63, no. 1, pp.653–664, Jan. 2016.
[34] M. Zaja, M. Oprea, C. G. Suarez, and L. Mathe, "Electric Vehicle Battery Charging Algorithm Using PMSM Windings and an Inverter as an Active Rectifier," in *2014 IEEE Vehicle Power and Propulsion Conference (VPPC)*, 2014, pp. 1–6.
[35] L. Wang, J. Liang, G. Xu, K. Xu, and Z. Song, "A novel battery charger for plug-in hybrid electric vehicles," in *2012 IEEE International Conference on Information and Automation*, 2012, pp. 168–173.
[36] Tiago J. C. Sousa, Luís Machado, Delfim Pedrosa, Vítor Monteiro, and João L. Afonso, "Unified Traction and Battery Charging Systems for Electric Vehicles: A Sustainability Perspective", in *2019 EAI International Conference on Sustainable Energy for Smart Cities (SESC)*, Braga, Portugal, 4-6 December 2019.
[37] M. Depenbrock, "The FBD-method, a generally applicable tool for analyzing power relations," *IEEE Transactions on Power Systems*, vol. 8, no. 2, pp. 381–387, May 1993.
[38] G. Albright, J. Edie, and S. Al-Hallaj, "A Comparison of Lead Acid to Lithium-ion in Stationary Storage Applications," *AllCell Technologies White Paper*, no. March, p. 14, 2012.
[39] B. B. McKeon, J. Furukawa, and S. Fenstermacher, "Advanced Lead–Acid Batteries and the Development of Grid-Scale Energy Storage Systems," *Proceedings of the IEEE*, vol. 102, no. 6, pp. 951–963, Jun. 2014.
[40] G. J. May, A. Davidson, and B. Monahov, "Lead batteries for utility energy storage: A review," *Journal of Energy Storage*, vol. 15, pp. 145–157, Feb. 2018.
[41] S. Jinlei, P. Lei, L. Ruihang, M. Qian, T. Chuanyu, and W. Tianru, "Economic Operation Optimization for 2nd Use Batteries in Battery Energy Storage Systems," *IEEE Access*, vol. 7, pp. 41852–41859, 2019.